Chemical Engineering Journal 153 (2009) 70–79

Contents lists available at ScienceDirect

Chemical Engineering Journal

journal homepage: www.elsevier.com/locate/cej

Removal of Ni(II), Cd(II), and Pb(II) from a ternary aqueous solution by amino functionalized mesoporous and nano mesoporous silica

Aghdas Heidari [a], Habibollah Younesi [a,*], Zahra Mehraban [b]

[a] Department of Environmental Science, Faculty of Natural Resources & Marine Science, Tarbiat Modares University, Imam Reza Street, P.O. Box 46414-356, Noor, Iran
[b] New Technologies Committee, Research Institution for Curriculum Development and Educational Innovations, Tehran, 1584634818, Iran

ARTICLE INFO

Article history:
Received 4 February 2009
Received in revised form 21 May 2009
Accepted 9 June 2009

Keywords:
Adsorption
NH_2-MCM-41
Nano NH_2-MCM-41
Isotherms

ABSTRACT

In the present study, the application for the removal of Ni(II), Cd(II) and Pb(II) ions from aqueous solution by using mesoporous silica materials, namely, MCM-41, nanoparticle of MCM-41, NH_2-MCM-41 (amino functionalized MCM-41) and nano NH_2-MCM-41 was investigated. Suitable adsorbents preparation techniques were developed in the laboratory. The effects of the solution pH, metal ion concentrations, adsorbent dosages, and contact time were studied. It was found that NH_2-MCM-41 showed the highest uptake for metal ions in aqueous solution. The results indicated that the adsorption of Ni(II), Cd(II) and Pb(II) ions on the surface of the adsorbent was increased with increasing solution pH. The experimental data were analyzed using the Langmuir and Freundlich equations. Correlation coefficients were determined by analyzing each isotherm. It was found that the Langmuir equation showed better correlation with the experimental data than the Freundlich. According to the parameters of the Langmuir isotherm, the maximum adsorption capacity of NH_2-MCM-41 for Ni(II), Cd(II) and Pb(II) was found to be 12.36, 18.25 and 57.74 mg/g, respectively. The kinetic data of adsorption reactions and the evaluation of adsorption equilibrium parameters were described by pseudo-first-order and pseudo-second-order equations. The synthesized solid sorbents were characterized by Fourier transform infrared (FT-IR) spectrometry, X-ray diffraction (XRD), scanning electron microscopy (SEM) and nitrogen sorption measurements.

© 2009 Published by Elsevier B.V.

1. Introduction

Industrial heavy metal pollution has become a serious environmental and sanitary problem all over the world in recent years. Heavy metals can not only have toxic and harmful effects on organisms living in water, but also accumulate throughout the food chain and may also affect human beings [1,2]. Heavy metals such as cadmium, lead and nickel among others, are commonly detected in industrial effluents. Cadmium is used in a wide variety of industrial processes such as alloy preparation, metal plating, mining, ceramics and other industrial activities [3]. A variety of syndromes, renal function hypertension, hepatic injury, lung damage and teratogenic effects may result from cadmium toxicity [4]. Lead pollution results from textile dying, ceramic and glass industries, petroleum refining, battery manufacture and mining operations [5]. Lead may cause mental disturbance, retardation, and semi-permanent brain damage [6]. The occurrence of heavy metals especially cadmium and nickel in industrial effluents beyond permissible limits brings serious environmental pollution, threatening human health and ecosystem [7]. Therefore, these pollutions must be removed to an acceptable level before being released into water ecosystem.

Many techniques, such as ion exchange, precipitation, adsorption, membrane processes, reverse osmosis, sedimentation, electro-dialysis, etc., have been employed for separation of heavy metals from wastewater [8,9]. With the increase in environmental pollution, there is a growing demand to develop novel adsorbents of higher efficiency for heavy metal ions removal from aqueous media than those commercially available [10]. Mesoporous silica materials have received considerable attention because of their unique large surface area, well-defined pore size and pore shape [11,12]. As one of these materials, MCM-41, consisting of hexagonal arrays of large and uniform pore size, large surface area, thermal stability and mild acidic property [13,14]. Mesoporous silica MCM-41 has been functionalized and employed to eliminate traces of toxic heavy metal from wastewater [15,16]. For environmental applications, the development of functionalized nanoporous material is necessary. Mostly, the functionalizations of mesoporous silica have been studied. For example, Yoshitake et al. [16] investigated the amino functionalized mesoporous silicas for removal of arsenate from a dilute aqueous solution. Lam et al. [15] prepared gold-selective adsorbent from mesoporous silica MCM-41 by grafting organic amine groups. Algarra et al. [17] evaluated the potential of removing nickel and copper from industrial electroplating wastewaters using

* Corresponding author. Tel.: +98 122 625 3101x3; fax: +98 122 625 3499.
E-mail addresses: hunesi@modares.ac.ir, hunesi@yahoo.com (H. Younesi).

1385-8947/$ – see front matter © 2009 Published by Elsevier B.V.
doi:10.1016/j.cej.2009.06.016

aminopropyl groups functional mesoporous silica MCM-41 materials. Furthermore, the adsorption selectivity of NH_2-MCM-41 for Ni(II) and Cd(II) ions in binary component adsorption was recently examined by Lam et al. [18] recently. However, the literature studies on the removal efficiency of functionalized mesoporous silica for Cd(II) and Pb(II) are very limited. Previous studies deal mostly with adsorption characteristics of some heavy metals including Cu, Ni, Hg, Au and As, especially with single component adsorption. The adsorption of Pb(II), Ni(II) and Cd(II) ions with nano MCM-41 and nano NH_2-MCM-41 in comparison with MCM-41 and NH_2-MCM-41 has not reported.

In this study, MCM-41 mesoporous silica was prepared under basic condition by using hexadecyltrimethylammoniumbromide as template and fumed silica as the silica source by means of hydrothermal method. Nano MCM-41 mesoporous silica was synthesized by the same template and tetraethoxysilane as the silica source by means of sol–gel method. The incorporation of amine functional groups into MCM-41 and nano MCM-41 mesoporous silica was successfully synthesized by a liquid phase grafting method. The application of MCM-41, NH_2-MCM-41, and nanoparticles of MCM-41 and, NH_2-MCM-41 for removal of Pb(II), Ni(II) and Cd(II) from aqueous solution was examined and compared. The effects of solution pH, contact time, metal ion concentrations and adsorbent dosages on the adsorption capacity of NH_2-MCM-41 were studied in order to analyze the adsorption kinetics and determine the equilibrium time. Langmuir and Freundlich isotherms were applied to the experimental equilibrium data in order to explain the adsorption mechanism. The adsorption kinetics of Pb(II), Ni(II) and Cd(II) ions by NH_2-MCM-41 was investigated for different concentrations of the metal ions at a constant adsorbent dosage and constant solution pH.

2. Materials and methods

2.1. Materials

Fumed silica (SiO_2), hexadecyltrimethylammoniumbromide (CTAB), n-hexane, $CdCl_2$, $Pb(NO_3)_2$ and $NiCl_2$ standard solutions and hydrochloric acid (37%) from Merck Co. (Germany), sodium hydroxide (NaOH) from Applichem (Germany), tetraethoxysilane (TEOS) and 3-aminopropyltrimethoxisilane (98%) from Sigma–Aldrich (USA) were purchased. All reagents were used in their analytical grade without further purification.

2.2. Synthesis of mesoporous silica MCM-41

MCM-41 was prepared according to the method of Mehraban and Farzaneh [19] using hydrothermal crystallization [4]. Fumed silica (0.03 mol) was added to a sodium hydroxide solution (0.6 M). The above mixture was stirred and heated for 3 h at 80 °C. The mixture was cooled down to room temperature. CTAB (0.015 mol) was added to the gel under vigorous stirring. The white solution was stirred vigorously for 1 h then 0.0102 mol of concentrated HCl (37%) was added dropwise followed by addition of 27 ml deionized water. The gel was agitated at room temperature for 2 h while stirring and then transferred into a Teflon bottle. The crystallization was performed for 3 days at 100 °C after which the material was filtered and washed with distilled water, dried at 100 °C overnight, and calcined for 2 h at 150 °C and for 6 h at 540 °C at a rate of 3 °C/min. The molar composition of the mixture was SiO_2:NaOH:CTAB:HCl:H_2O = 1:0.54:0.50:0.34:100.

2.3. Synthesis of NH_2-MCM-41

NH_2-MCM-41 was prepared according to the method of Ho et al. [20]. In 50 ml of n-hexane, 2.5 g of calcined MCM-41 and 2.5 g of 3-aminopropyltrimethoxisilane were refluxed for 6 h. The mixture was filtered, washed with n-hexane (20 ml), dried at room temperature and stored in a desiccator. The schematic route of functionalized MCM-41 mesoporous silica is shown in Fig. 1.

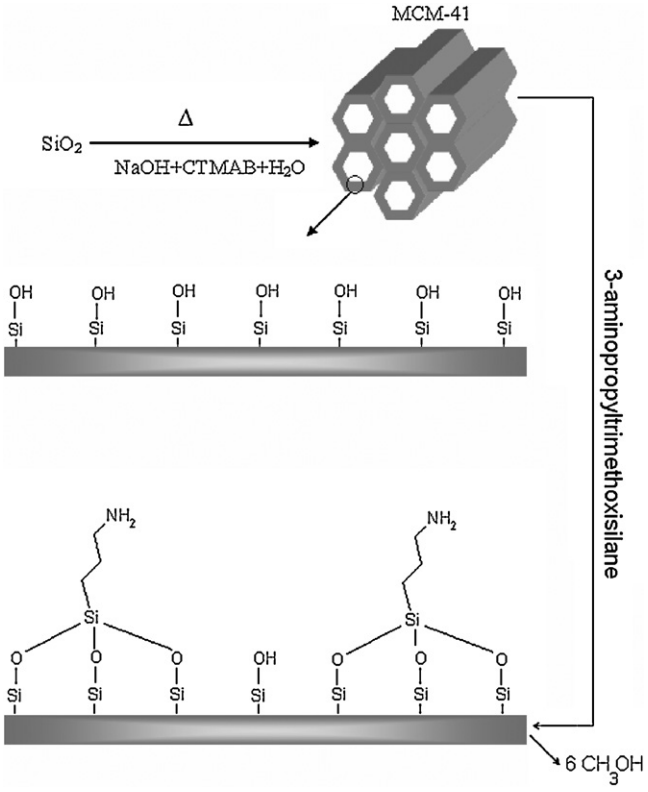

Fig. 1. Schematic functionalization route of MCM-41 mesoporous silica.

2.4. Synthesis of nano MCM-41

Nanoparticles of MCM-41 were prepared using sol–gel method according to Cai et al. [21]. CTAB (3.75 mmol) was added to the solution of NaOH (9.3 mmol in 646.5 ml of distilled water). The obtained mixture was stirred while heating at 80 °C. Then TEOS (30 mmol) was added dropwise into the above homogeneous mixture giving white slurry after 2 h. The resulting product was filtered and washed with distilled water, dried at room temperature and calcination was carried out at 550 °C for 4 h. The molar composition of the mixture was H_2O:NaOH:CTAB:TEOS = 1197:0.31:0.125:1.

2.5. Synthesis of nano NH_2-MCM-41

Nano NH_2-MCM-41 was prepared according to the method of Ho et al. [20]. Calcined nanoparticles of MCM-41 (2.5 g) were refluxed in 50 ml of n-hexane containing 2.5 g of 3-aminopropyltrimethoxisilane for 6 h. The powder of the nanoparticles of NH_2-MCM-41 was filtered, washed with n-hexane (20 ml) and dried at room temperature overnight.

2.6. Preparation of standard solutions

Atomic absorption spectrometry standard solutions of 1000 mg/l Ni(II), Cd(II) and Pb(II) were used for adsorption experiments. Working standards were prepared from the dilution of stock solutions every day. All aqueous solutions were prepared by de-ionized water with conductivity <1 μmho/cm at room temperature. The adsorption experiments were carried out in a batch scale mode.

The pH of the solutions was adjusted to desired values using either NaOH (0.1 M) or HCl (0.1 M) solutions.

2.7. Characterization

X-ray diffraction (XRD) patterns of the silica were obtained by XRD diffractometer (X'pert, Philips, Holland) which was operated at an acceleration voltage of 40 kV by using Cu Kα radiation (λ = 1.54 Å). Infrared spectra were recorded on a Fourier transform infrared (FT-IR) spectrometer (Shimadzo, FTIR1650 spectrophotometer, Japan) in the range of 400–4000 cm^{-1} using spectroscopic quality KBr powder (sample/KBr = 1/100). The structure and morphology of nanoparticles of MCM-41 were examined by electron scanning microscopy (SEM, Phillips XL30, Holland). The textural properties of the MCM-41 including surface area, pore volume, and pore size distribution were determined by nitrogen adsorption–desorption isotherms (ASAP 2010). Surface areas were calculated by the Brunauer–Emmet–Teller (BET) equation, and pore sizes were estimated by identifying the highest peaks in the distribution of pore size, which were calculated by non-local density functional theory (NLDFT). The concentrations of metal ions of the solutions were measured by atomic absorption spectroscopy (AAS, Philips, PU9400, USA).

2.8. Effect of variable parameters on the adsorption process of metal ions

2.8.1. Effect of contact time

The analysis of batch adsorption of metal ion was carried out in 10 min steps and the concentration of each sample was measured by atomic absorption spectroscopy after 120 min contact time. The data for adsorption experiment were replicated three times and the results were averaged. The standard deviation was less than 5%. The results were recorded and the time profile of heavy metal ions adsorption was plotted.

2.8.2. Effect of adsorbent dose

The ternary component adsorption of Ni(II), Cd(II), and Pb(II) was studied using mesoporous silica MCM-41 (0.5, 1 and 2 g) and NH_2-MCM-41 (0.0125, 0.05, 0.125, 0.25, 0.5, 1 and 2 g), nanoparticles of MCM-41 (0.5, 1 and 2 g) and nanoparticles NH_2-MCM-41 (0.0125, 0.05, 0.125, and 0.25, 0.5, 1 and 2 g) in a 250 ml Erlenmeyer flasks containing 100 ml aqueous solution of 50 mg/l Ni(II), Cd(II), and Pb(II). The pH was adjusted to 5.0 by adding 0.1 M NaOH. The batch adsorption experiments were carried out under stirring at 150 rpm at room temperature for 120 min contact time. The samples were centrifuged (236 HK, Hermle, German) at 16,000 rpm for 10 min at 25 °C and subsequently filtered with 0.45 μm filter paper (Whatman) to remove and recover the adsorbent.

2.8.3. Effect of solution pH

A sample of NH_2-MCM-41 (0.5 g) was suspended in 100 ml of 50 mg/l of Ni(II), Cd(II), and Pb(II) at several pH values (1.5, 2.5, 3.5 and 5.0) using either 0.1 M NaOH or 0.1 M HCl. These samples were stirred for 120 min at 150 rpm. Then the samples were centrifuged at 16,000 rpm for 10 min at 25 °C and filtered with 0.45 μm filter papers to remove and recover the adsorbent. The percent of removed metal ions by the adsorbents was calculated by the following equation:

$$R = \frac{C_0 - C_t}{C_0} \times 100 \quad (1)$$

where R is the removal efficiency of the metals ions, C_0 is the initial concentration of the metal ions in mg/l, and C_t is the concentration of the metal ions at any time in mg/l.

2.9. Equilibrium adsorption study

The equilibrium adsorption capacity of adsorbent was calculated by the following equation:

$$q_e = \frac{(C_0 - C_e)V}{W} \quad (2)$$

where q_e is the equilibrium adsorption capacity of adsorbent in mg metal/g adsorbent, C_0 is the initial concentration of the metal ions in mg/l, C_e is the equilibrium concentration of metal ions in mg/l, V is the volume of metal ions solution in l, and W is the weight of the adsorbent in g. The equilibrium adsorption of metals ions solutions by NH_2-MCM-41 was measured (100 ml of 10–70 mg/l) after 120 min contact time.

2.10. Adsorption isotherms

The equilibrium adsorption data of Ni(II), Pb(II), and Cd(II) ions were fitted into both the Freundlich and Langmuir isotherm equations. In the Langmuir model, it is assumed that the adsorption surface sites have identical energy and each adsorbate molecule has been located on a single site and hence this model predicts the formation of monolayer of a adsorbate on the adsorbent surface [22]. The Langmuir isotherm is given as:

$$q_e = \frac{q_m b C_e}{1 + bC_e} \quad (3)$$

where q_e is the equilibrium sorption capacity of sorbent in mg metal/g sorbent, C_e is the equilibrium concentration of metal ions in mg/l, q_m is the maximum amount of metal sorbed in mg metal/g sorbent, and b is the constant that refers to the bonding energy of sorption in l/mg. Nonlinear regression analysis was performed in SigmaPlot software (SigmaPlot 6.0, SPSS Inc., USA) in order to estimate the values of q_m and b parameters.

The Freundlich model describes a reversible heterogeneous adsorption since it does not restrict itself to a monolayer of adsorbent covering [23]. Actually, the Freundlich isotherm predicts that the heavy metal ion concentration on the adsorbent will increase as long as there is an increase of the ion concentration in the liquid solution [24]. The Freundlich isotherm is given as:

$$q_e = K_f C_e^{1/n} \quad (4)$$

where q_e is the equilibrium adsorption capacity of the adsorbent in mg metal/g adsorbent, C_e is the equilibrium concentration of heavy metal ions in mg/l, K_f is the constant related to the adsorption capacity of the adsorbent in mg/l, and n is the constant related to the adsorption intensity of the adsorbent. Nonlinear regression analysis was carried out by SigmaPlot software (SigmaPlot 6.0, SPSS Inc., USA) in order to predict the K_f and n parameters.

2.11. Adsorption kinetics

To test the experimental data, the controlling mechanisms of adsorption processes were investigated according to pseudo-first-order and pseudo-second-order kinetic equations. In order to analyze the uptake rates of ions, a simple kinetic analysis using the pseudo-first-order equation was done [25,26]. The pseudo-first-order kinetic model is given as [27]:

$$\log(q_e - q_t) = \log q_e - \frac{K_1}{2.303} t \quad (5)$$

where q_e and q_t are the amount of metal ions adsorbed on the adsorbent in mg/g at equilibrium and at time t, respectively, and K_1 is the constant of first-order adsorption in min^{-1}. The pseudo-second-

order kinetic model is given as [28].

$$\frac{t}{q_t} = \frac{1}{K_2 q_e^2} + \frac{t}{q_e} \quad (6)$$

where K_2 is the rate constant of second-order adsorption in g mg^{-1} min^{-1}. The equilibrium sorption capacity, the pseudo-first-order rate constant and the pseudo-second-order rate constant were determined experimentally from the slope and the intercept of straight-line plots of Eqs. (5) and (6), in order to obtain the applicability of these kinetic models to fit the experimental data.

2.12. Desorption experiments

In order to estimate the recovery of Cd(II), Ni(II) and Pb(II) from NH_2-MCM-41, desorption experiments with different reagents (H_2SO_4, HCl and HNO_3 solutions) were performed at several pH values (0.5, 1.0, and 2.0). Solutions of Cd(II), Ni(II) and Pb(II) of 100 ml with initial concentration of 50 mg/l and 0.5 g of NH_2-MCM-41 were shaken at 150 rpm at 25 °C. After 120 min the adsorbent was separated by centrifugation (at 3000 rpm for 10 min) and the residual solid was dried at 40 °C. Then the obtained solid phase mass was added to 100 ml of the effluent. Samples were collected after 5, 10, 30, 60 and 120 min contact time with the effluent to evaluate metal recovery. The metal recovery was calculated by the following equation:

$$\text{Metal recovery} = \frac{\text{Amount of metal ions desorbed}}{\text{Amount of metal ions adsorbed}} \times 100 \quad (7)$$

3. Results and discussions

3.1. Characterization of adsorbents

Fig. 2 shows the X-ray diffraction (XRD) patterns of MCM-41, NH_2-MCM-41, nano MCM-41 and nano NH_2-MCM-41. The XRD pattern of MCM-41 showed three diffraction peaks that can be indexed to (1 0 0), (1 1 0) and (2 0 0) in the 2θ range from 0.8 to 10°. A strong diffraction peak in the low-angle region (2θ = 2.09–2.10°) is associated with the (1 0 0) reflection of hexagonal cell. Apart from this intense peak, we can observe two additional weak peaks which can be indexed to the (1 1 0) and (2 0 0) reflections of the typical hexagonal cell indicating that the amine grafted sample preserves the mesoscopic order after a functionalization process. The low-angle XRD diffractions of NH_2-MCM-41 (Fig. 2a) compared with MCM-41 (Fig. 2b) correspond to the materials grafted with amine groups. From Fig. 2a, it can be seen that the phase of nano NH_2-MCM-41 still preserve the morphology of hexagonal structure. The broad diffraction peak of the nano MCM-41 indicates relatively small size, which is probably due to the mesoporous silica in the final product (Fig. 2c). These observations constitute a clear proof for the existence of highly ordered hexagonal pore systems. The estimated hexagonal pore diameters from d_{100} values are listed in Table 1. As it can be seen, the pore size distribution and the mean cell diameter are relatively narrow. However, the high surface area was found for the MCM-41 nanoparticles. From the above results it can be deduced that the nanoparticles improve the surface area of mesoporous silica, which is an important factor for grafting with amine groups.

Table 1
Characterization data of MCM-41.

Molecular sieves	S_{BET}[a] (m^2/g)	a°[b] (nm)	d_{100} (Å)
MCM-41	966	4.85	42.01
Nano MCM-41	1387	4.88	42.22

[a] BET surface area.
[b] Unit cell diameter that calculated from XRD data ($a^\circ = 2d_{100}/3^{1/2}$).

The results of N_2 sorption experiments and estimated pore diameters by XRD data are listed in Table 1. The specific surface area, pore size distribution and total pore volume of the materials were calculated by the Brunauer–Emmet–Teller (BET) equation. It is noticeable that in nano MCM-41, due to the particles becoming smaller in size, the surface area was higher. MCM-41 was a porous material with surface area of 966 m^2/g and mean pore diameter of 4.85 nm, while the surface area of nano MCM-41 was 1387 m^2/g.

The FT-IR spectra of the four samples are shown in Fig. 3. The broad absorption band in the region 3765–3055 cm^{-1} can be attributed to the stretching of the framework Si–OH group with the defective sites and physically adsorbed water molecules (Fig. 3a). The vibrations of Si–O–Si can be seen at 1095 cm^{-1} (asymmetric stretching), 814 cm^{-1} (symmetric stretching) and 460 cm^{-1} (bending) [29,30]. After functionalization with amine group, NH_2-MCM-41 and nano NH_2-MCM-41 show visible broad absorption bands at 1560 cm^{-1} and at 1650 cm^{-1} corresponding to the bending vibration of N–H group, while N–H stretching (3200–3500 cm^{-1})

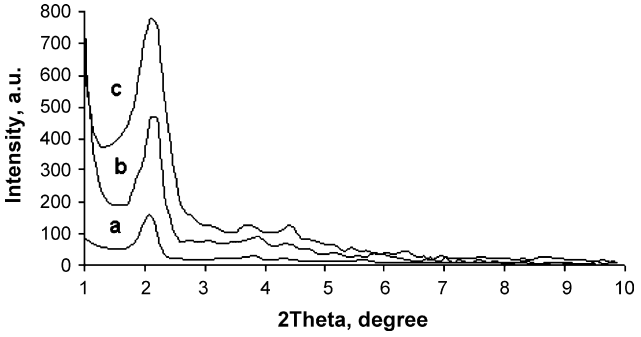

Fig. 2. XRD patterns of (a) NH_2-MCM-41, (b) MCM-41, (c) nano MCM-41 and (d) nano NH_2-MCM-41.

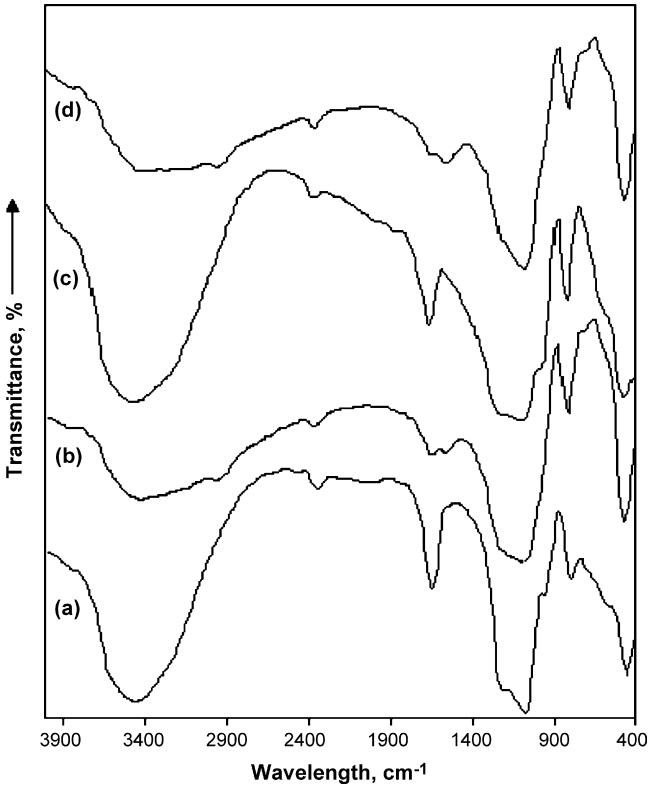

Fig. 3. FT-IR spectra of (a) MCM-41 (b) NH_2-MCM-41 (c) nano MCM-41 and (d) nano NH_2-MCM41.

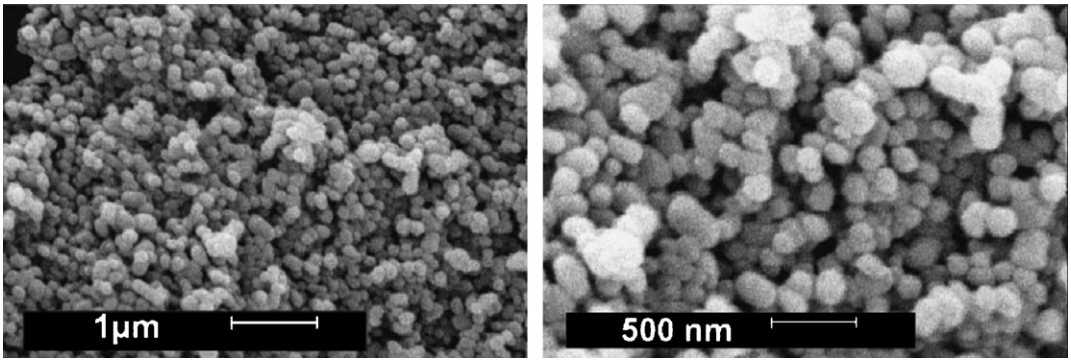

Fig. 4. SEM images of nanometer MCM-41 at (left) low and (right) high magnification.

and C–N stretching (1030–1230 cm^{-1}) overlap with the broad absorption band of the silanol group and the Si–O–Si vibrations (Fig. 3b). The FT-IR band distribution of MCM-41 (Fig. 3a) was similar to nano MCM-41 (Fig. 3c), which indicates that they had similar surface chemical properties. As evidenced by FT-IR, the surface chemical properties of NH_2-MCM-41 (Fig. 3b) were much more like nano NH_2-MCM-41 (Fig. 3d). They also indicate how changes are induced by grafting of amine functionality to MCM-41 mesoporous silica, which shows stretching vibration of N–H and C–H groups. Therefore, the synthesis of a weak base anion exchanger with a primary amine group is responsible for the chelating of Cd(II), Ni(II) and Pb(II) and the adsorption was assumed to be established by the complex formation reaction between Cd(II), Ni(II) and Pb(II) and the nitrogen atom in the functional groups.

Fig. 4 shows the scanning electron microscopy images of nano MCM-41. There are clear similarities between the lower (Fig. 4a) and the higher magnification (Fig. 4b). It is clearly revealed that the mesoporous nanoparticles preserved the spherical morphology for the silica template as shown in Fig. 4a. According to the high-magnification SEM image, the size distribution of spherical particle of nano MCM-41 is mainly in the range 60–80 nm as shown in Fig. 5. The formation of MCM-41 in nanoparticle can be attributed to its higher surface area than that of MCM-41.

3.2. Adsorption studies

3.2.1. Effect of adsorbent dose

In order to compare the removal efficiency of Ni(II), Cd(II), and Pb(II) ions, the effect of the doses of MCM-41, NH_2-MCM-41, nano MCM-41, and nano NH_2-MCM-41 is shown in Fig. 6. It was found that the adsorption of Ni(II), Cd(II), and Pb(II) from ternary aqueous solution increased with increasing adsorbent dose due to increasing of interference between binding sites at higher sorbent dosages or insufficiency of metal ions in solution with respect to available

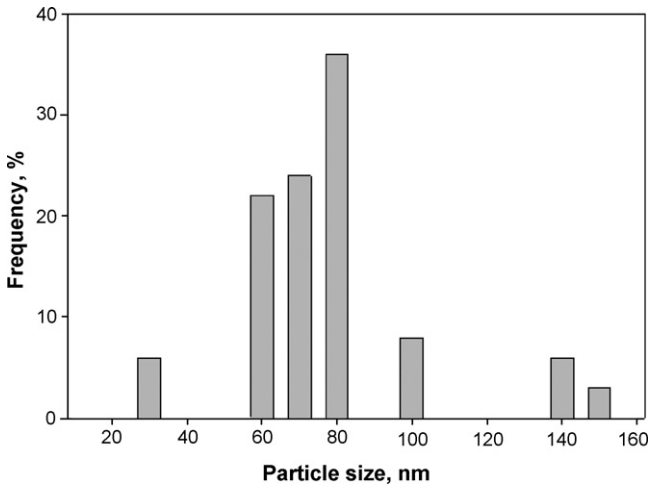

Fig. 5. The particle size distribution of nano MCM-41.

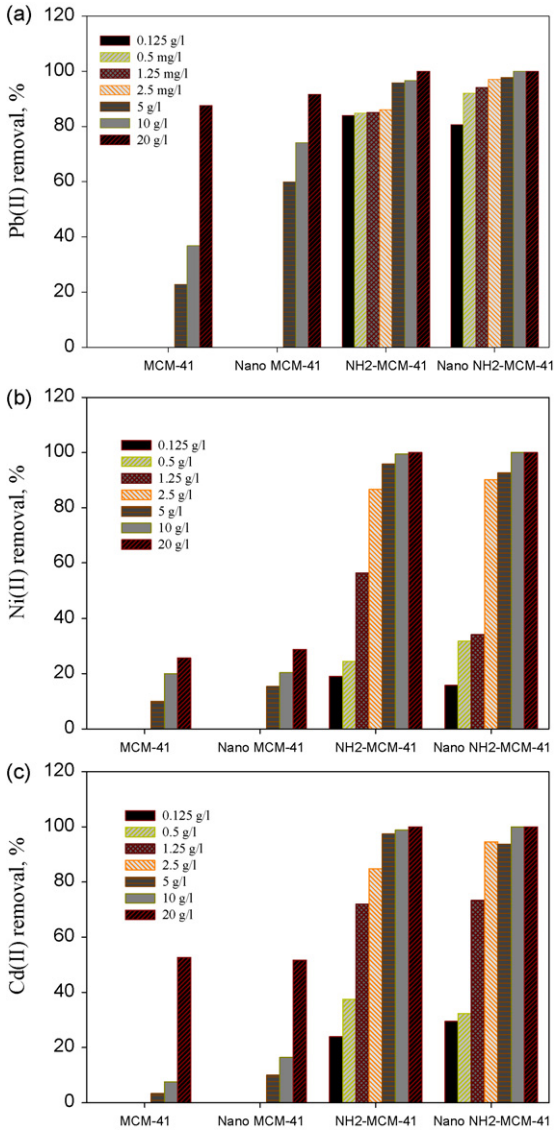

Fig. 6. Effect of adsorbent dose on the removal efficiency in a ternary system adsorption by NH_2-MCM-41 (a) Pb(II), (b) Ni(II), and (c) Cd(II).

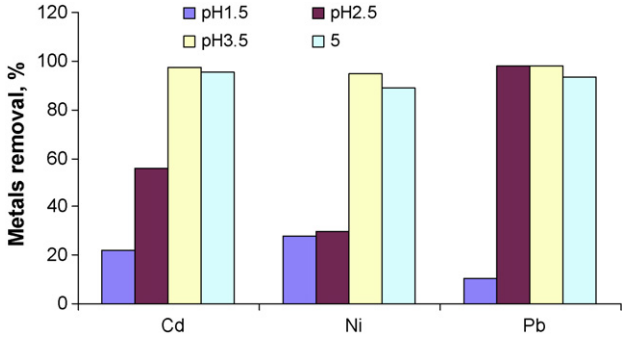

Fig. 7. Effect of pH on Cd(II), Ni(II) and Pb(II) removal onto NH_2-MCM-41: operated at metals concentration of 50 mg/l, NH_2-MCM-41 dose of 5 g/l, ambient temperature of 25 °C, and contact time of 2 h.

binding sites [31]. Fig. 1a, b and c shows that the 5 g/l of MCM-41 can remove 8.2% Ni(II), 2.8% Cd(II), and 29% Pb(II) from aqueous solution whereas, nano MCM-41 could remove 15% Ni(II), 47% Cd(II), and 75% Pb(II). Furthermore, NH_2-MCM-41 was able to remove 92% Ni(II), 93% Cd(II), and 95% Pb(II) at a dosage of 5 g/l (Fig. 1a–c). In addition, nano NH_2-MCM-41 shows 92% Ni(II), 93% Cd(II), and 97% Pb(II) removal at a dosage of 5 g/l (Fig. 1a–c). The reason for why nano MCM-41 has a larger removal compared to MCM-41 might be due to the larger specific surface area of nano MCM-41. However, NH_2-MCM-41 and nano NH_2-MCM-41 had the maximum adsorption of Ni(II), Cd(II) and Pb(II) because the amino groups on NH_2-MCM-41 and nano NH_2-MCM-41 interact with heavy metal ions by complexion mechanism which is necessary for removing them from aqueous solution.

3.2.2. Effect of solution pH

The effect of the solution pH on the sorption of Cd(II), Ni(II), and Pb(II) metal ions by NH_2-MCM-41 is shown in Fig. 7. It was found that the sorption efficiency increased with increase in the solution pH from 1.5 to 5.0. It means that the adsorption of metal ions depends on the solution pH, which influences electrostatic binding of ions to corresponding $-NH_2$ groups decreasing the solution pH values; as the protonated amine groups to varied degrees were increased [17], the number of binding sites available for Cd(II), Ni(II) and Pb(II) ions uptake were then decreased. Consequently the extent of Cd(II), Ni(II) and Pb(II) ions uptake was low in the high concentrations of protons. With increasing pH, $-NH_2$ groups were de-protonated and forming negatively charged sites [23,32,33]. At pH values higher than 6.0, Pb(II) ions precipitated out because of the high concentrations of –OH ions in the aqueous solution [32,34,35]. The adsorption capacity of NH_2-MCM-4 for Cd(II) adsorption increased with the increase of the solution pH. But the adsorption capacity of NH_2-MCM-41 for Ni(II) and Pb(II) adsorption first increased from pH 1.5 to 3.5, then decreased when the pH value reached 5.0.

3.2.3. Isothermal models and adsorption kinetics

Removal of single heavy metal ions of Ni(II), Cd(II) and Pb(II) using NH_2-MCM-41 is affected by several factors. These factors include the specific surface properties of the adsorbent and the physicochemical parameters of the solution such as temperature, pH, initial heavy metal ions concentration, and adsorbent dose. Many other parameters affect the capacity of NH_2-MCM-41 to bind more than one metal ions simultaneously. The combined effects of two or more metal ions to NH_2-MCM-41 also depend on the number of metal species competing for binding sites, metal ions combination and levels of metal ions concentration [36–38].

In order to predict the adsorption behaviors of Ni(II), Pb(II) and Cd(II) ions solution onto NH_2-MCM-41, Langmuir and Freundlich isotherms are used (Fig. 8). The b, q_m, n, K_f values and the nonlinear regression correlations for Langmuir (R^2) and Freundlich (R^2) are given in Table 2. The adsorption capacities (q_m, mg/g) using Langmuir isotherm equation were as follows: Pb(II) (57.74) > Cd(II) (18.25) > Ni(II) (12.36). The maximum adsorption capacity was observed for Pb(II) by NH_2-MCM-41 due to the physicochemical properties of Pb(II), which has the higher atomic weight, electronegativity, electrode potential and ionic size higher than Cd(II) and Ni(II) [39]. The Langmuir isotherm model shows that the b value of Cd(II) ion is higher than those of Ni(II) and Pb(II) ions, indicating that the adsorption energy of Cd(II) ion is higher than those of Ni(II) and Pb(II) ions. Comparing their nonlinear correlation coefficients, listed in Table 2, indicated that Langmuir model should describe the adsorption behaviors of Ni(II), Cd(II) and Pb(II) ions on the NH_2-MCM-41, especially for the Cd(II) ion better. Thus the Langmuir isotherm fits the experimental data better in

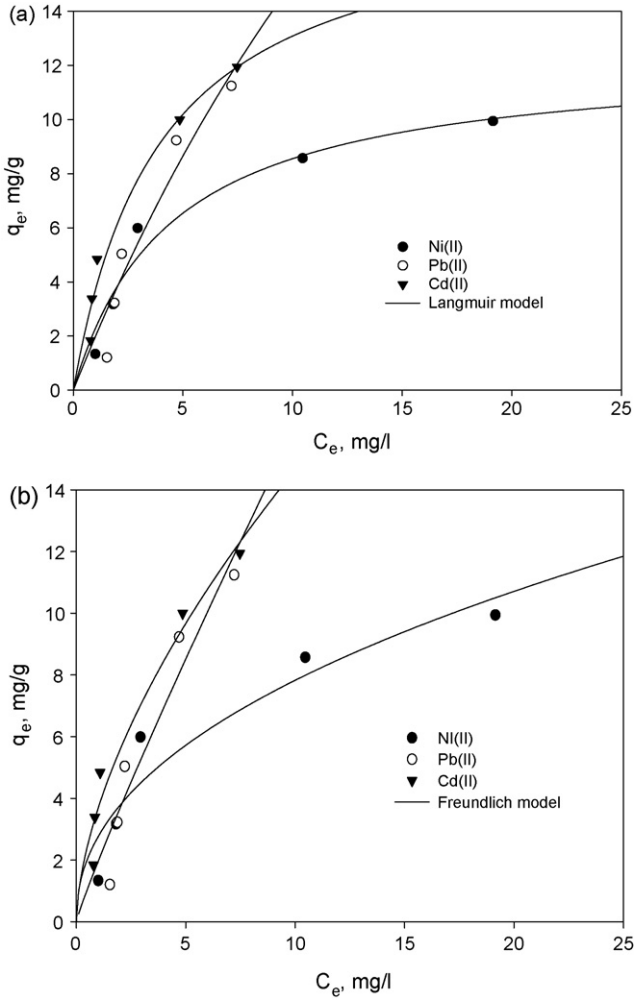

Fig. 8. Adsorption isotherm of Ni(II), Pb(II), and Cd(II) onto NH_2-MCM-41 (a) Langmuir and (b) Freundlich.

Table 2
Adsorption parameters of the Langmuir and Freundlich isotherms at room temperature for the adsorption of Ni(II), Cd(II) and Pb(II) on NH2-MCM-41.

Metals	Langmuir			Freundlich		
	q_m (mg/g)	b (l/mg)	R^2	K_f	n	R^2
Ni	12.36	0.2245	0.9569	2.759	2.209	0.9009
Cd	18.25	0.2526	0.9703	3.680	1.666	0.9588
Pb	57.74	0.0352	0.9248	1.958	1.095	0.9173

Table 3
Comparison of the adsorption capacity of silica-based adsorbents.

Adsorbents	Absorbent dose (g/l)	Metal ion concentration	Solution pH	Ligand (moiety)	q_m (mmol/g) (mg/g)			Ref.
					Cd^{2+}	Ni^{2+}	Pb^{2+}	
MCM-41		–		–OH	0	0	–	[18]
NH_2-MCM-41	1	3 mM	5	$–RNH_2$	0.71 (79.8)	0.69 (40.5)	–	[18]
NH_2-MCM-41[a]	1	3 mM	5	$–RNH_2$	0.56 (63)	0.15 (8.8)	–	[18]
Functionalized porous silica	10	–	6	Aminopropyl ($H_2N(CH_2)_3$ [amino-ethylamino]propropyl (H_2N-$(CH_2)_2$-$NH(CH_2)_3$) 2-aminoethylamino)ethylamino]propyl ($H_2N(CH_2)_2$-NH-$(CH_2)_2$-$NH(CH_2)_3$–)	0.1	0.015	–	[45]
	10	–	6			0.001	–	
	10	–	6		0.01	0.15	–	
	10	–	6	Mercaptopropyl (HS-$(CH_2)_3$–)	0.2	0.005	–	
NH_2-MCM-41[b]	5	50 mg/l	5	$–NH_2$	(18.25)	(12.36)	(57.74)	This work

[a] Binary component adsorption.
[b] Ternary component adsorption.

contrast to Freundlich may be due to the homogenous distribution of active sites on the NH_2-MCM-41 surface, since the Langmuir equation assumes that the surface is homogenous and all sites have equal adsorption energies [34,40].

Table 2 demonstrates that MCM-41 sorbents exhibit different adsorption capacities for Ni(II) and Cd(II) ions, which indicates that the property of a grafted functional group at the surface of sorbents and the presence of the other heavy metal ions in solution play important roles in the maximum adsorption capacity of Ni(II), Pb(II) and Cd(II) ions. It was also found that the adsorption capacity of Ni(II) and Cd(II) ions onto MCM-41 is very small (Table 2). It has been reported that functional MCM-41 chemically modified by amine and SH groups exhibits much better adsorption capacity for Ni(II) and Cd(II) ions [41]. However, functional MCM-41 chemically modified by an amine group exhibits much better adsorption ability for Ni(II) and Cd(II) ions. NH_2-MCM-41 exhibit standing adsorption efficiency for these ions. One of the important factors that have an effect on the adsorption capacity of NH_2-MCM-41 for Ni(II) and Cd(II) ions is the presence of the other heavy metal ions in solution [19]. Comparing the adsorption capacity exhibited in our work with those of silica-based adsorbents reported by other authors (Table 3) indicates that the presence of the other heavy metal ions in solution (single, binary and ternary component adsorption) decreases the maximum adsorption capacity of Ni(II) and Cd(II) ions. The dimensionless separation factor R_L can predict the affinity between the sorbate and adsorbent. When the R_L values lie between 0 and 1, the adsorption isotherm is favorable [42].

$$R_L = \frac{1}{1 + C_0 b} \tag{8}$$

where b is the Langmuir constant in l/mg and C_0 is the initial concentration of metal ions in mg/l. The R_L classified as $R_L > 1$, $0 < R_L < 1$ and $R_L = 0$ suggests that adsorption is unfavorable, favorable and irreversible, respectively. The values of R_L for adsorption of Cd(II), Ni(II) and Pb(II) ions onto NH_2-MCM-41 are shown in Fig. 9. These results indicate that the adsorption of Cd(II), Ni(II) and Pb(II) ions by NH_2-MCM-41 is more favorable at higher initial metal ion concentrations than at lower ones.

3.2.4. Adsorption kinetics

Kinetics of the adsorption process is vital in wastewater treatment, as it provides essential information on the reaction pathways and the solute uptake rate. In order to investigate the rate of metal ions sorption, the linear form of pseudo-first-order and pseudo-second-order kinetics was applied to the obtained results as shown in Figs. 10 and 11. The parameters of the pseudo-first-order and

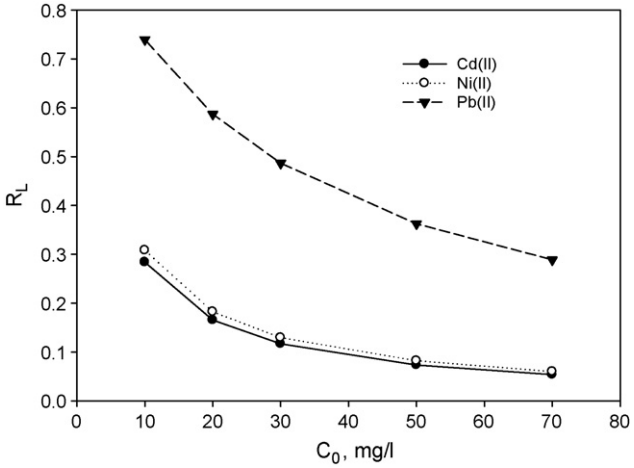

Fig. 9. Values of R_L for adsorption of Cd(II), Ni(II) and Pb(II) ions onto NH_2-MCM-41.

Table 4
Kinetic adsorption parameters obtained using Pseudo-first-order and Pseudo-second-order models.

Metals	Metal concentration (mg/l)	Pseudo-first-order			Pseudo-second-order		
		K_1	q_{e1}	R^2	K_2	q_{e2}	R^2
Cd(II)	10	0.184	1.84	0.9057	0.502	1.86	0.9995
	20	0.137	3.40	0.8863	0.282	3.43	0.9995
	30	0.108	4.90	0.9933	0.050	5.10	0.9948
	50	0.063	10.01	0.9871	0.010	10.86	0.9894
	70	0.036	12.43	0.9791	0.005	13.83	0.9705
Pb(II)	10	–	–	–	14.861	1.15	0.9987
	20	–	–	–	13.373	3.22	0.9999
	30	–	–	–	2.741	5.10	0.9999
	50	–	–	–	5.331	9.23	0.9999
	70	–	–	–	0.181	11.89	0.9999
Ni(II)	10	0.095	1.34	0.9859	–	–	–
	20	0.057	3.34	0.9574	–	–	–
	30	0.024	6.31	0.9384	–	–	–
	50	0.022	13.02	0.9440	–	–	–
	70	0.015	16.65	0.9600	–	–	–

pseudo-second-order sorption kinetics model are listed in Table 4. The measured coefficient values of the pseudo-second-order model exceeded 0.97 and the calculated sorption capacity values obtained from pseudo-second-order model were more consistent with the experimental values of sorption capacity. Therefore, the pseudo-second-order model represented better the sorption kinetics of Cd(II) ion implying that Cd(II) adsorption onto NH_2-MCM-41 may take place through a chemical process involving valence forces through sharing or exchange of electrons [43].

According to Fig. 10a and b, sorption mechanism of the pseudo-first-order model for Cd(II) and Ni(II) onto NH_2-MCM-41 shows reasonable agreement with the experimental data. However, in the pseudo-first-order model for Pb(II) ion the measured regression correlation was low, the plots of $\log(q_e - q_t)$ versus time were not presented. In this case, the experimental values of q_e are not in good agreement with the calculated theoretical values of q_e in Eq. (5). It can be concluded that the sorption mechanism of Pb(II) ion onto NH_2-MCM-41 does not follow the pseudo-first-order kinetic

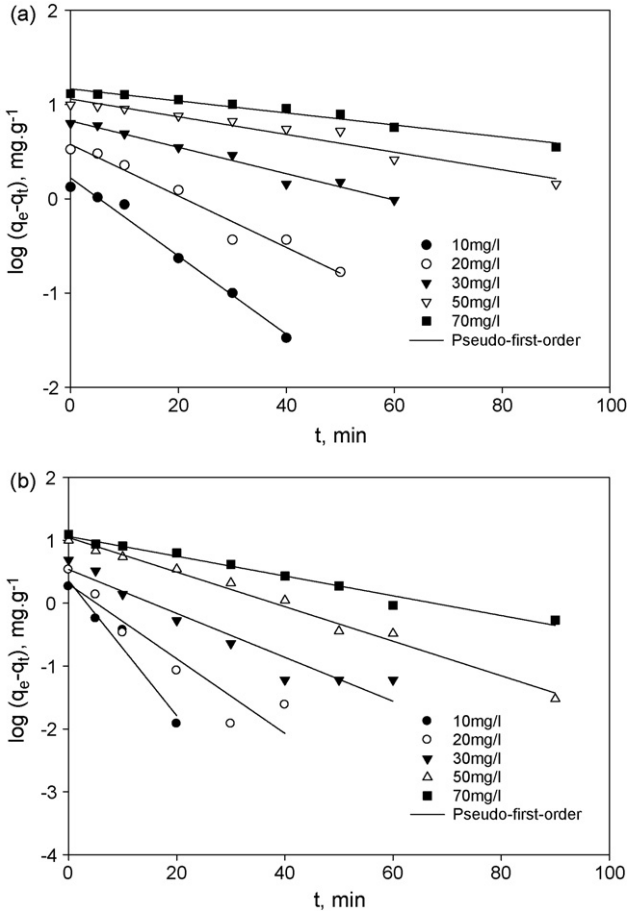

Fig. 10. Pseudo-first-order kinetic for adsorption of (a) Ni(II) and (b) Cd(II) onto NH_2-MCM-41.

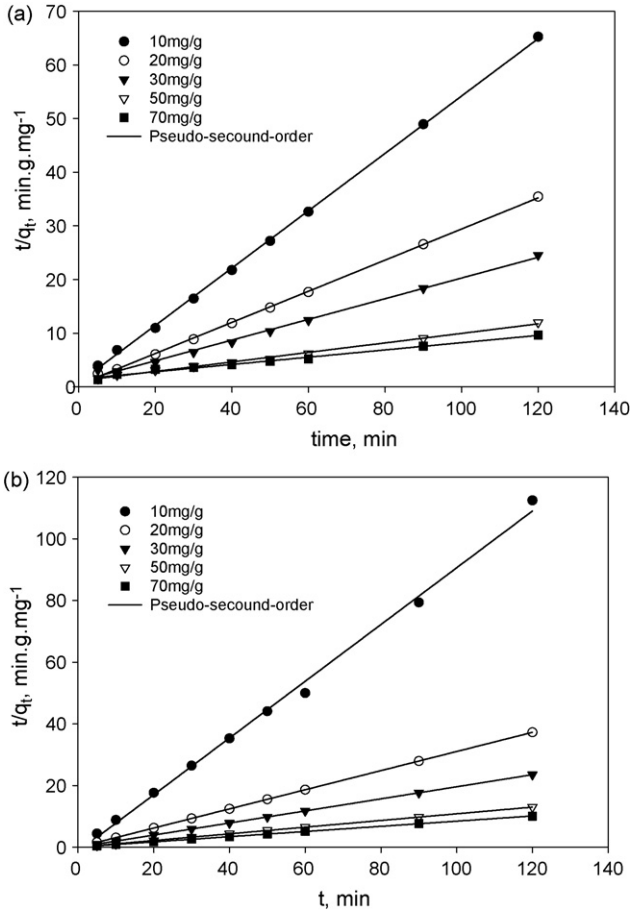

Fig. 11. Pseudo-second-order kinetic adsorption onto NH_2-MCM-41 (a) Cd(II) and (b) Pb(II).

model. Therefore, the pseudo-first-order model is not suitable for modeling the sorption of Pb(II) onto NH_2-MCM-41. Furthermore, the experimental data were tested by the pseudo-second-order kinetic model, and based on the regression correlations (above 0.9705), good agreement exists between our results for Cd(II) and Pb(II), as shown in Fig. 11a and b. Many studies reported that the first-order equation does not fit well to the initial stages of the adsorption processes. The first-order kinetic processes have been used for reversible reactions with an equilibrium being established between liquid and solid phases [44]. Whereas, the pseudo-second-order kinetic model assumes that chemical adsorption may be the rate-limiting step [27,44].

3.2.5. Desorption

Sorbents recovery is most important in the assessment of the competitiveness of adsorption systems. The adsorption reversibility of Cd(II), Ni(II) and Pb(II) ions onto NH_2-MCM-41 was studied by three kinds of effluents at three different concentrations. Cd(II), Ni(II) and Pb(II) ions adsorbed onto NH_2-MCM-41 were effectively eluted out by using HCl, H_2SO_4 and HNO_3 as an eluents. The results reveal that the desorption efficiency of Cd(II), Ni(II) and Pb(II) ions increased with the increase in the concentration of eluents. The best result was achieved with HCl (100 mmol/l) that can apparently act as an effective desorption effluent. In the case of this experiment, the amount of desorption efficiency was up to 90%. The removal efficiency of desorption increased also when the concentration of the eluents was increased. The adsorption–desorption cycle results demonstrated that the NH_2-MCM-41 could be reused up to 5 times without a significant change in the amount of adsorption for studied metal ions. Therefore, there are good prospects for NH_2-MCM-41 in practical applications for the removal of Ni(II), Cd(II) and Pb(II) from water and wastewater.

4. Conclusion

In the present study, as a fundamental study on the reprocessing of heavy metal polluted wastewater by the adsorption method, mesoporous organically modified silica-based materials of about 70 nm in particle size functionalized with primary amine groups were synthesized. Synthesized mesoporous materials, namely MCM-41, NH_2-MCM-41, nano MCM-41, and nano NH_2-MCM-41 were examined in a ternary component adsorption experiment for investigating their capacity in heavy metal adsorbents to remove Ni(II), Cd(II) and Pb(II) from aqueous solution. The results suggest that the adsorption is influenced by the solution pH, the concentration of the metal ions, dosages of adsorbents and contact time. The optimized pH was 5 for adsorption of Cd(II), Ni(II) and Pb(II) ions on NH_2-MCM-41. It was found that NH_2-MCM-41 showed the best uptake for Ni(II), Cd(II) and Pb(II) ions and the Langmuir model is the best model to describe Cd(II), Ni(II) and Pb(II) ions adsorption behavior onto NH_2-MCM-41. The maximum adsorption capacity values of Ni(II), Cd(II) and Pb(II) ions in a ternary component adsorption with NH_2-MCM-41 (from Langmuir equation) were 12.36, 18.25 and 57.74 mg/g, respectively. The kinetic data justified that the adsorption of Cd(II) and Pb(II) ions onto NH_2-MCM-41 followed the pseudo-second-order kinetic model and the kinetic adsorption of Ni(II) was described by the pseudo-first-order model. The kinetic studies indicated that the contact time was suitable for the technological applications. The adsorption–desorption cycle results described in the subject paper open an important area for future applications of the mesoporous organically modified silica-based materials. Therefore, there are good prospects for NH_2-MCM-41 for the removal of Ni(II), Cd(II) and Pb(II) ions from water and wastewater in practical applications. Consequently, fundamentally the outlook is promising that the amine functionalized mesoporous silica MCM-41 has the potential of removing significant amounts of metal ions from aqueous solutions.

Acknowledgements

The study was supported through a research grant from the Ministry of Science, Iran, and the Tarbiat Modares University (TMU). The authors wish to thank Mrs. Haghdoust for her assistance (Technical Assistant of Environmental Laboratory), Ellen Vuosalo Tavakoli for the English editing, and the Faculty of Natural Resources and Marine Sciences, Tarbiat Modares University and Ministry of Science for their financial support.

References

[1] R.J.E. Martins, R. Pardo, R.A.R. Boaventura, Cadmium(II) and zinc(II) adsorption by the aquatic moss *Fontinalis antipyretica*: effect of temperature, pH and water hardness, Water Res. 38 (2004) 693–699.
[2] A. Sarl, M. Tuzen, Biosorption of cadmium(II) from aqueous solution by red algae (*Ceramium virgatum*): equilibrium, kinetic and thermodynamic studies, J. Hazard. Mater. 157 (2008) 448–454.
[3] T.A. Davis, B. Volesky, R.H.S.F. Vieira, Sargassum seaweed as biosorbent for heavy metals, Water Res. 34 (2000) 4270–4278.
[4] A. Sari, D. Mendil, M. Tuzen, M. Soylak, Biosorption of Cd(II) and Cr(III) from aqueous solution by moss (*Hylocomium splendens*) biomass: equilibrium, kinetic and thermodynamic studies, Chem. Eng. J. 144 (2008) 1–9.
[5] O.M.M. Freitas, R.J.E. Martins, C.M. Delerue-Matos, R.A.R. Boaventura, Removal of Cd(II), Zn(II) and Pb(II) from aqueous solutions by brown marine macro algae: kinetic modelling, J. Hazard. Mater. 153 (2008) 493–501.
[6] A.T. Paulino, L.B. Santos, J. Nozaki, Removal of Pb2+, Cu2+, and Fe3+ from battery manufacture wastewater by chitosan produced from silkworm chrysalides as a low-cost adsorbent, React. Funct. Polym. 68 (2008) 634–642.
[7] M. Amini, H. Younesi, N. Bahramifar, Biosorption of nickel(II) from aqueous solution by *Aspergillus niger*: response surface methodology and isotherm study, Chemosphere 75 (2009) 1483–1491.
[8] D. Pérez-Quintanilla, A. Sánchez, I. del Hierro, M. Fajardo, I. Sierra, Preparation, characterization, and Zn2+ adsorption behavior of chemically modified MCM-41 with 5-mercapto-1-methyltetrazole, J. Colloid Interface Sci. 313 (2007) 551–562.
[9] M. Amini, H. Younesi, N. Bahramifar, Statistical modeling and optimization of the cadmium biosorption process in an aqueous solution using *Aspergillus niger*, Colloids Surf. Physicochem. Eng. Aspects 337 (2009) 67–73.
[10] M.M. Matlock, K.R. Henke, D.A. Atwood, Effectiveness of commercial reagents for heavy metal removal from water with new insights for future chelate designs, J. Hazard. Mater. 92 (2002) 129–142.
[11] C.T. Kresge, M.E. Leonowicz, W.J. Roth, J.C. Vartuli, J.S. Beck, Ordered mesoporous molecular sieves synthesized by a liquid-crystal template mechanism, Nature 359 (1992) 710–712.
[12] J.S. Beck, J.C. Vartuli, W.J. Roth, M.E. Leonowicz, C.T. Kresge, K.D. Schmitt, C.T.W. Chu, D.H. Olson, E.W. Sheppard, et al., A new family of mesoporous molecular sieves prepared with liquid crystal templates, J. Am. Chem. Soc. 114 (1992) 10834–10843.
[13] S. Morin, P. Ayrault, S. El Mouahid, N.S. Gnep, M. Guisnet, Particular selectivity of m-xylene isomerization over MCM-41 mesoporous aluminosilicates, Appl. Catal. A: Gen. 159 (1997) 317–331.
[14] N. Kumar, V. Nieminen, L.E. Lindfors, T. Salmi, D.Y. Murzin, E. Laine, T. Heikkilä, Cu-H-MCM-41, H-MCM-41 and Na-MCM-41 mesoporous molecular sieve catalysts for isomerization of 1-butene to isobutene, Catal. Lett. 78 (2002) 105–110.
[15] K.F. Lam, K.L. Yeung, G. McKay, An investigation of gold adsorption from a binary mixture with selective mesoporous silica adsorbents, J. Phys. Chem. B 110 (2006) 2187–2194.
[16] H. Yoshitake, T. Yokoi, T. Tatsumi, Adsorption behavior of arsenate at transition metal cations captured by amino-functionalized mesoporous silicas, Chem. Mater. 15 (2003) 1713–1721.
[17] M. Algarra, M.V. Jiménez, E. Rodríguez-Castellón, A. Jiménez-López, J. Jiménez-Jiménez, Heavy metals removal from electroplating wastewater by aminopropyl-Si MCM-41, Chemosphere 59 (2005) 779–786.
[18] K.F. Lam, K.L. Yeung, G. McKay, Efficient approach for Cd2+ and Ni2+ removal and recovery using mesoporous adsorbent with tunable selectivity, Environ. Sci. Technol. 41 (2007) 3329–3334.
[19] Z. Mehraban, F. Farzaneh, MCM-41 as selective separator of chlorophyll-a from β-carotene and chlorophyll-a mixture, Micropor. Mesopor. Mater. 88 (2006) 84–90.
[20] K.Y. Ho, G. McKay, K.L. Yeung, Selective adsorbents from ordered mesoporous silica, Langmuir 19 (2003) 3019–3024.
[21] Q. Cai, Z.S. Luo, W.Q. Pang, Y.W. Fan, X.H. Chen, F.Z. Cui, Dilute solution routes to various controllable morphologies of MCM-41 silica with a basic medium, Chem. Mater. 13 (2001) 258–263.
[22] H.L. Vasconcelos, T.P. Camargo, N.S. Gonçalves, A. Neves, M.C.M. Laranjeira, V.T. Favere, Chitosan crosslinked with a metal complexing agent: synthesis, characterization and copper(II) ions adsorption, React. Funct. Polym. 68 (2008) 572–579.

[23] F. Ghorbani, H. Younesi, S.M. Ghasempouri, A.A. Zinatizadeh, M. Amini, A. Daneshi, Application of response surface methodology for optimization of cadmium biosorption in an aqueous solution by *Saccharomyces cerevisiae*, Chem. Eng. J. 145 (2008) 267–275.
[24] J.C.P. Vaghetti, E.C. Lima, B. Royer, B.M. da Cunha, N.F. Cardoso, J.L. Brasil, S.L.P. Dias, Pecan nutshell as biosorbent to remove Cu(II), Mn(II) and Pb(II) from aqueous solutions, J. Hazard. Mater. 162 (2009) 270–280.
[25] M.K. Durjava, T.L. ter Laak, J.L.M. Hermens, J. Struijs, Distribution of PAHs and PCBs to dissolved organic matter: high distribution coefficients with consequences for environmental fate modeling, Chemosphere 67 (2007) 990–997.
[26] T.L. terLaak, M. Durjava, J. Struijs, J.L.M. Hermens, Solid phase dosing and sampling technique to determine partition coefficients of hydrophobic chemicals in complex matrixes, Environ. Sci. Technol. 39 (2005) 3736–3742.
[27] P. Ding, K.-L. Huang, G.-Y. Li, W.-W. Zeng, Mechanisms and kinetics of chelating reaction between novel chitosan derivatives and Zn(II), J. Hazard. Mater. 146 (2007) 58–64.
[28] Y.S. Ho, G. McKay, Pseudo-second order model for sorption processes, Process Biochem. 34 (1999) 451–465.
[29] J.R. Sohn, S.J. DeCanio, J.H. Lunsford, D.J. O'Donnell, Determination of framework aluminium content in dealuminated Y-type zeolites: a comparison based on unit cell size and wavenumber of i.r. bands, Zeolites 6 (1986) 225–227.
[30] V. Umamaheswari, M. Palanichamy, V. Murugesan, Isopropylation of m-Cresol over mesoporous Al-MCM-41 molecular sieves, J. Catal. 210 (2002) 367–374.
[31] L. Rome, G.M. Gadd, Copper adsorption by *Rhizopus arrhizus*, *Cladosporium resinae* and *Penicillium italicum*, Appl. Microbiol. Biotechnol. 26 (1987) 84–90.
[32] M. Amini, H. Younesi, N. Bahramifar, A.A.Z. Lorestani, F. Ghorbani, A. Daneshi, M. Sharifzadeh, Application of response surface methodology for optimization of lead biosorption in an aqueous solution by *Aspergillus niger*, J. Hazard. Mater. 154 (2008) 694–702.
[33] A. SarI, M. Tuzen, Kinetic and equilibrium studies of biosorption of Pb(II) and Cd(II) from aqueous solution by macrofungus (*Amanita rubescens*) biomass, J. Hazard. Mater. 164 (2009) 1004–1011.
[34] O. Altin, O.H. Ozbelge, T. Dogu, Effect of pH, flow rate and concentration on the sorption of Pb and Cd on montmorillonite. I. Experimental, J. Chem. Technol. Biotechnol. (1999) 1131–1138.
[35] A. Sari, M. Tuzen, D. Citak, M. Soylak, Equilibrium, kinetic and thermodynamic studies of adsorption of Pb(II) from aqueous solution onto *Turkish kaolinite* clay, J. Hazard. Mater. 149 (2007) 283–291.
[36] E. Deliyanni, N. Lazaridis, E. Peleka, K. Matis, Metals removal from aqueous solution by iron-based bonding agents, Environ. Sci. Pollut. Res. 11 (2004) 18–21.
[37] Z. Matějka, H. Parschová, L. Jelínek, E. Mištová, P. Houserová, P. Ruszová, F. Šebesta, Selective removal of As, Sb, Se and Be from water streams; screening of uptake mechanisms and sorbent-types, J. Ion Exchange 14 (2003) 237–240.
[38] T. Erwe, V. Mavrov, H. Chmiel, Characterization of a synthetic zeolite P as a heavy metal bonding agent, Chem. Pap. 57 (2003) 45–49.
[39] I.A. Sengil, M. Özacar, Competitive biosorption of Pb^{2+}, Cu^{2+} and Zn^{2+} ions from aqueous solutions onto valonia tannin resin, J. Hazard. Mater. 166 (2009) 1488–1494.
[40] M. Özacar, I.A. Sengil, Adsorption of metal complex dyes from aqueous solutions by pine sawdust, Bioresour. Technol. 96 (2005) 791–795.
[41] K. Ariga, A. Vinu, J.P. Hill, T. Mori, Coordination chemistry and supramolecular chemistry in mesoporous nanospace, Coord. Chem. Rev. 251 (2007) 2562–2591.
[42] A. Bhatnagar, A.K. Jain, A comparative adsorption study with different industrial wastes as adsorbents for the removal of cationic dyes from water, J. Colloid Interface Sci. 281 (2005) 49–55.
[43] Y.S. Ho, G. McKay, Sorption of dyes and copper ions onto biosorbents, Process Biochem. 38 (2003) 1047–1061.
[44] K.S. Low, C.K. Lee, S.C. Liew, Sorption of cadmium and lead from aqueous solutions by spent grain, Process Biochem. 36 (2000) 59–64.
[45] L. Bois, A. Bonhommé, A. Ribes, B. Pais, G. Raffin, F. Tessier, Functionalized silica for heavy metal ions adsorption, Colloids Surf. Physicochem. Eng. Aspects 221 (2003) 221–230.